Validation of a drift diffusion model for a hollow cathode

IEPC-2019-914

Presented at the 36th International Electric Propulsion Conference
University of Vienna • Vienna, Austria
September 15-20, 2019

Stephen B. Gabriel[1]
University of Southampton, Southampton, Hampshire, SO17 1BJ, England

Abstract: There are only 2 complete 2-D axisymmetric models for space hollow cathodes. Both include coupling to thermal models and give good results when compared with the rather sparse data on experimental results (3) and also include modelling of the three regions, internal, orifice and plume. However, these models are custom built and not readily available. COMSOL has been used previously for an SPT 100 hollow cathode running on xenon and achieved reasonably good results when compared to the available limited experimental data on anode voltages and internal pressures, which did not include detailed plasma parameters such as the electron density, temperature and potentials in the insert, orifice and plume regions. More recently, preliminary simulations have been performed using the drift diffusion model and laminar(compressible) flow interfaces from COMSOL with argon propellant for both static gas experiments on a heaterless hollow cathode and more conventional orificed cathodes. Whilst preliminary results appeared to be physically plausible for both cases, the simulations did not seem to be robust with respect to changes in geometry and pressure leading to non-convergence. This paper continues these preliminary studies, presenting further modelling results which focus on the validation of a COMSOL model with xenon by comparing with both the published model results and experimental results for one operating condition of the NSTAR hollow cathode. The COMSOL predictions are in good overall agreement with other recent models throughout nearly all of the regions and compare well with the experimental measurements in the insert region. The paper will present more detailed results on the plasma characteristics, highlight some of the problems with using Cosmol and potential solutions along with some of the reasons between the differences between the Comsol results, the experimental measurements and other predictions.

Nomenclature

R_e = source term
α_j = Townsend coefficient for reaction j (m2)
$\boldsymbol{\Gamma_e}$ = electron flux(m-2s-1)
R_ε = electron energy loss term
j*k* = diffusive flux vector
Rk = the rate expression for species *k* (SI unit: kg/(m3·s))
u =is the mass averaged fluid velocity vector (SI unit: m/s)
wk = the mass fraction of the *k*th species
$\Delta\varepsilon_j$ = energy loss from the reaction j
ρ = density of the mixture (SI unit: kg/m3)

[1] Professor of Aeronautics and Astronautics, Electronics and Computer Science Department, sbg2@soton.ac.uk

ρ_q	=	space charge density
γ_p	=	the secondary emission coefficient

I.INTRODUCTION

Despite having been around for more than 40 years or more, space hollow cathodes are not completely understood due to the complexity of the plasma physics involved, the small dimensions which makes measurements inside problematic and the coupling of the thermal design with that of the flow and plasmas. If in addition, the presence of sheaths at boundaries with thermionic emission and wear due to erosion of the orifice, sublimation or vaporisation of the insert in the case of LaB6 and complex thermochemical changes of the surface and Ba loss in the case of BaO dispenser inserts, then it's understandable that there are still unanswered questions. Despite this much progress has been made both in terms of simulation and experimental measurements. The JPL model (1,2) and their experimental measurements of the interior plasma (2) have increased our understanding significantly as well as the fidelity of plasma simulations. More recently there has been the development of a coupled thermal and plasma model (3, 4) which yields good results when compared with measurements.

However, unless one has access to these powerful, custom made numerical models, the design of a hollow cathode is still very much empirical with perhaps some semi-empirical rules of thumb to help.

The motivation for this paper was initially driven by the idea that perhaps, existing commercially available software might be able to help in the design of a heaterless hollow cathode. First attempts were at modelling of the cathode and keeper discharge with static gas using simplified geometries. The 2-D discharge plasma tool within COMSOL was used with Argon gas. Later, attempts were made at modelling a more conventional orificed hollow cathode with gas flow, similar to those performed for an SPT 100 hollow cathode running on xenon (5) but were inconclusive and appeared not to show any promise. Refinement of the model was continued with the inclusion of more details of the thermionic emission at the emitter wall and the use of xenon rather than argon as the propellant. Since the initial results looked reasonable, it was decided to try to validate the model using the same technique that was utilised in (3), that is to compare the model results with the on-axis measurements of electron density, temperature and plasma potential for the NSTAR cathode at one specific operating point, namely TH15.

The paper begins with a brief summary of the COMSOL model used, including the boundary conditions and neutral flow followed by some of the results with an emphasis on a comparison with the results from (3) and the experimental measurements (2). In the final section, conclusions are drawn on the suitability of such a COMSOL model an engineering design tool, it's capability of predicting keeper potentials and future work.

II.THE COMSOL MODEL

B. EQUATIONS

The 2-D discharge model in the COMSOL Plasma Applications Library is used.
This is essentially a drift diffusion model which solves the following equations(domain):

$$\frac{\partial}{\partial t}(n_e) + \nabla\cdot\,[-n_e(\boldsymbol{\mu_e}\cdot\boldsymbol{E}) - \boldsymbol{D_e}\cdot\,\nabla n_e] = R_e \qquad (1)$$

$$\frac{\partial}{\partial t}(n_e) + \nabla\cdot\,[-n_e(\boldsymbol{\mu_\varepsilon}\cdot\boldsymbol{E}) - \boldsymbol{D_e}\cdot\,\nabla n_e] + \boldsymbol{E}\,\cdot\,\boldsymbol{\Gamma_e} = R_e \qquad (2)$$

where

$$\boldsymbol{\Gamma_e} = -(\boldsymbol{\mu_e}\cdot\boldsymbol{E})n_e - \boldsymbol{D_e}\cdot\,\nabla n_e \qquad (3)$$

To calculate the electron diffusivity, energy mobility and energy diffusivity the electron mobility is used:

$$\boldsymbol{D_e} = \boldsymbol{\mu_e}T_e, \boldsymbol{\mu_\varepsilon} = \left(\frac{5}{3}\right)\boldsymbol{\mu_e}, \boldsymbol{D_\varepsilon} = \boldsymbol{\mu_\varepsilon}T_e \qquad (4)$$

Townsend coefficients are used to calculate the source term, R_e using:

$$R_e = \sum_{j=1}^{M} x_j \alpha_j N_n |\boldsymbol{\Gamma_e}| \quad (5)$$

where α_j is the Townsend coefficient for reaction j (m2) and $\boldsymbol{\Gamma_e}$ is the electron flux(m-2s-1). The electron energy loss is calculated by summing the collisional energy losses for all the reactions to give

$$R_\varepsilon = \sum_{j=1}^{P} x_j k_j N_n \Delta\varepsilon_j \quad (6)$$

where $\Delta\varepsilon_j$ is the energy loss from the reaction j. Using Townsend coefficients, the electron energy loss is given by

$$R_\varepsilon = \sum_{j=1}^{P} x_j \alpha_j N_n |\boldsymbol{\Gamma_e}| \Delta\varepsilon_j \quad (7)$$

For the heavy particles, the mass fraction of each species is found from the transport equation :

$$\rho \frac{\partial}{\partial t}(\omega_k) = \rho(\boldsymbol{u} \cdot \nabla)\omega_k = \nabla \cdot \boldsymbol{j}_k + R_k \quad (8)$$

where

- $\mathbf{j}_k$ is the diffusive flux vector
- R_k is the rate expression for species k (SI unit: kg/(m3·s))
- **u** is the mass averaged fluid velocity vector (SI unit: m/s)
- ρ denotes the density of the mixture (SI unit: kg/m3), and
- ω_k is the mass fraction of the kth species (1).

Further details of this COMSOL interface can be found in the COMSOL plasma manual. For the electric potential the equations utilised are:

$$-\nabla \cdot \varepsilon_0 \varepsilon_r \nabla V = \rho_q \quad (9)$$

$$\rho_q = q\left(\sum_{k=1}^{N} Z_k n_k - n_e\right) \quad (10)$$

where the space charge density, ρ_q ,is automatically calculated from the model plasma chemistry using equation (10).

C. BOUNDARY CONDITIONS

The boundary conditions for the electron flux are given by:

$$\boldsymbol{n} \cdot \Gamma_{\boldsymbol{e}} = \left(\frac{1}{2} v_{e,th} n_e\right) - \sum_p \gamma_p (\Gamma_p \cdot \boldsymbol{n}) \quad (11)$$

and for the electron energy flux:

$$\boldsymbol{n} \cdot \Gamma_{\boldsymbol{\varepsilon}} = \left(\frac{5}{6} v_{e,th} n_\varepsilon\right) - \sum_p \varepsilon_p \gamma_p (\Gamma_p \cdot \boldsymbol{n}) \quad (12)$$

where γ_p is the secondary emission coefficient and the second term on the RHS of equation (11) gives the increase in electrons. ε_p is the mean energy of the secondary electrons with the second term in equation (12) giving the secondary emission energy flux.

Since ions are lost to the walls due to surface reactions and the electric field is directed towards the wall, the heavy particle equation becomes:

$$\boldsymbol{n} \cdot \boldsymbol{j}_k = M_\omega R_k + M_\omega c_k Z \mu_k (E \cdot \boldsymbol{n})[Z \mu_k (E \cdot \boldsymbol{n}) > 0] \quad (13)$$

D. PLASMA CHEMISTRY

The xenon gas modelled with the electronically excited states being combined into one single species, resulting in 3 species and 6 reactions as shown in Table 1 below

Table. 1

Reaction	Formula	Type	Δε(eV)
1	e+Xe=>e+Xe	Elastic	0
2	e+Xe=>e+Xes	Excitation	8.32
3	e+Xes=>e+Xe	Superelastic	-8.32
4	e+Xe=>2e+Xe+	Ionisation	12.13
5	e+Xes=>2e+Xe+	Ionisation	3.8
6	Xe+Xes=>e+Xe+Xe+	Penning ionisation	-

Surface reactions are shown in Table 2:

Table. 2

Reaction	Formula	Sticking coefficient	Secondary electron emission coefficient
1	Xes=>Xe	1	0
2	Xe+=>Xe	1	0.00 or 0.02

E. OTHER COMSOL SETTINGS

Different options are available for the two metal contacts, the keeper and the anode , with the cathode itself being grounded. The option which specifies current was used with the solution giving the potentials on the electrodes.

The mass flow is set at the inlet of the cathode and a pressure of 10Pa set at the outlet of the enclosing chamber. A temperature distribution is set on the insert wall and an energy for the emitted electrons; the COMSOL laminar flow(spf) was selected with coupling to the plasma model through the convection velocity and the absolute pressure.

No systematic study of mesh effects was carried out though different mesh sizes were tried including physics controlled and custom selected.

III. RESULTS

A. INTRODUCTION

The initial goal was to validate the model in the same way as (3), by calculating the profiles on axis of the electron density and temperature and plasma potential for the NSTAR cathode at the operating condition called TH15. To do this, the NSTAR discharge cathode geometry was modelled in a simplified way as shown in Figure 1. An open keeper, with the same orifice and external diameter and separation from the cathode tip as the NSTAR cathode, was used initially but later attempts were made to simulate closed keeper configurations. A cylindrical anode with an internal radius of 5cm was used.   Operating conditions corresponding to TH15 were selected, namely a mass flow rate of 3.6 sccm, a keeper current of 1.5A and an anode discharge current of 13A(2). It should be noted that for TH15 the keeper is actually floating or tied to the anode with a 1kohm resistor(6) and this is pointed out in (4). Since there is no thermal model, the temperature distribution along the length of the insert was assumed to be the measured one as was also done in (3) and is shown in Figure 2.

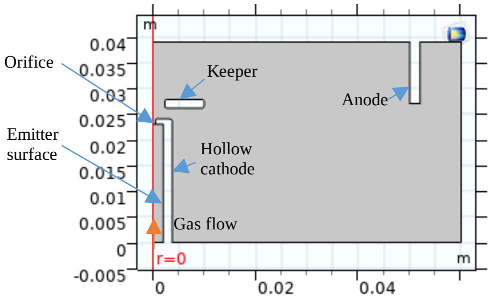

Figure 1. Simplified Geometry of Hollow Cathode

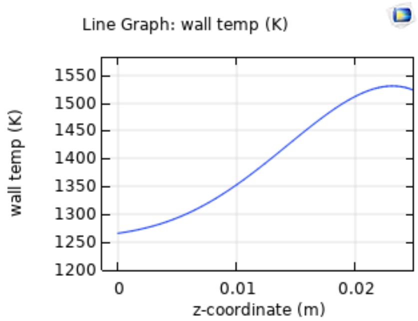

Figure 2. Temperature profile of emitter surface

B. Results

1. Plasma properties and neutral flow

Figures 3, 4 and 5 show 2-D colour coded plots of the electron density, plasma potential and electron temperatures.

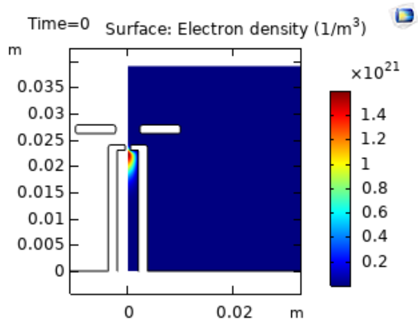

Figure 3 2-D electron density distribution

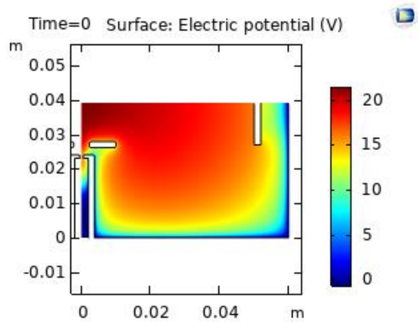

Figure 4 2-D potential distribution

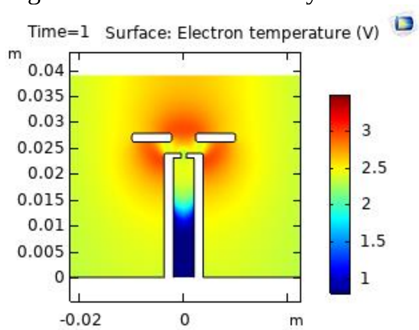

Figure 5 2-D electron temperature distribution

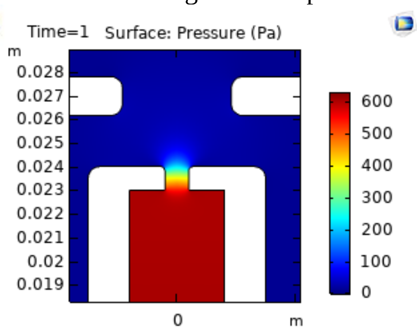

Figure 6 2-D pressure distribution

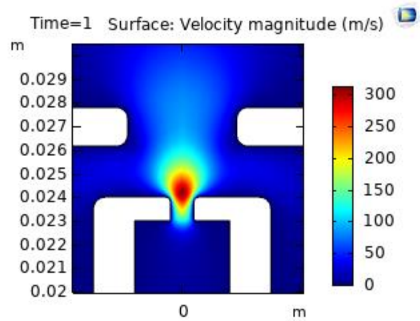

Figure 7 2-D Velocity distribution

Key points to note are that the plasma density is only identifiable into the inside of the hollow cathode cavity for about 3mm, showing a maximum value of about 1.4 x 10^{21} m^{-3} and strong radial gradients.
Figure 6 and 7 show colour coded plots of the pressure and flow velocity(magnitude). The key features are the essentially uniform pressure of about 10 Pa everywhere except inside the cathode itself and just outside the orifice of the cathode and similarly for the velocity magnitude where there is a large increase just before the cathode orifice entrance and then a sharp fall from just outside that orifice to a low value of about 100 m/s at the exit to the keeper orifice. These can be more clearly seen in Figures 8 and 9 where the low drop in pressure and corresponding small increase in velocity due to the laminar flow inside the cathode up to the cathode orifice entrance are identifiable. The pressure in the cathode interior is about 600 Pa or 4.5 Torr, which is of the same order as measured and calculated values published in the literature.

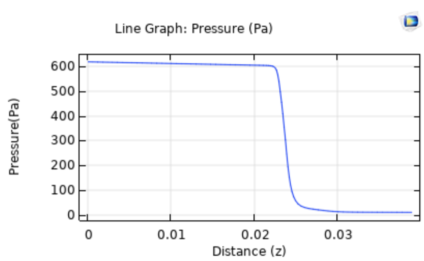

Figure 8. Axial pressure profile

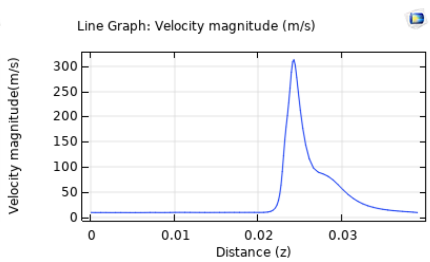

Figure 9. Axial velocity(magnitude)

2. Comparison with JPL measurements and Sary modelling

Figures 10, 11 and 12 show graphs of the on-axis values of the electron density, plasma potential and electron temperature as a function of the axial distance z, where the entrance to the cathode orifice is located at z=3cm.

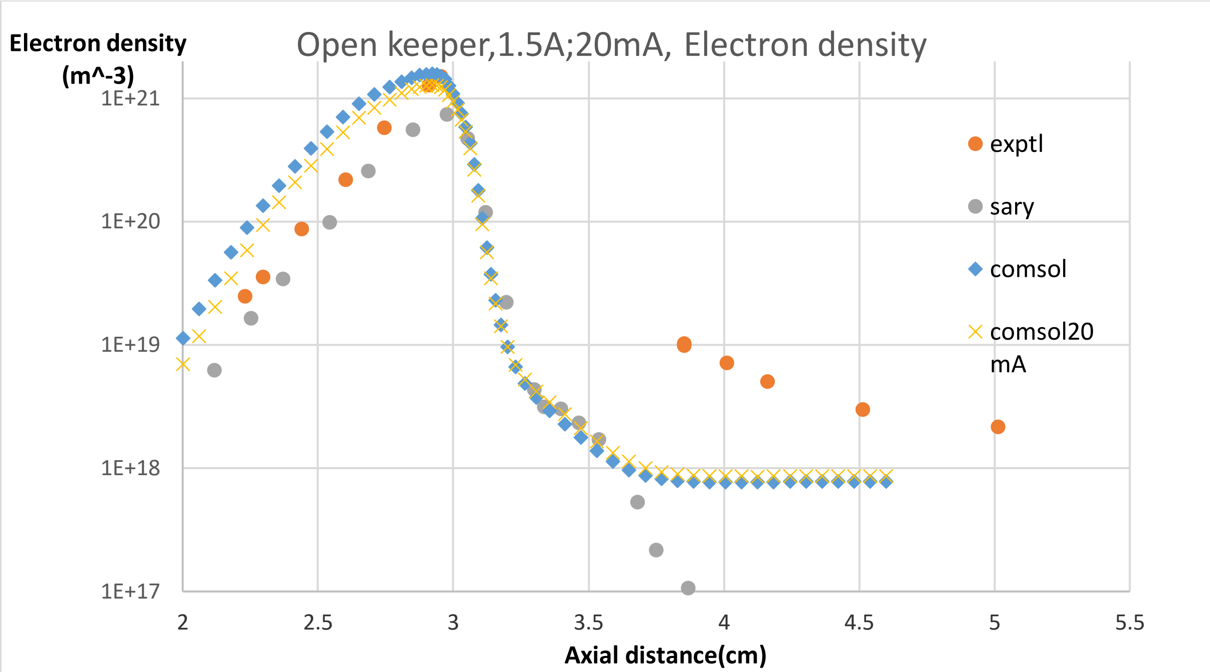

Figure 10. Comparison of electron densities on axis

For the electron densities as shown in Figure 10, there is good qualitative agreement between the Comsol results and both the experimental measurements and predictions from (3) with very similar trends. Upstream of the orifice the predicted densities tend to be higher than both the experimental and Sary predictions while the peak density is almost exactly the same as that measured experimentally(experimental 1.58e21m-3 versus 1.5e21m-3. Downstream of the cathode orifice until about 3.7cm, the Cosmol predictions are in excellent agreement with those from (3); beyond that distance the Comsol values tend to plateau whilst those of Sary continue to fall off and the experimental values continue to fall but more slowly and are significantly greater than both of the modelling predictions. As discussed in (3) this is thought to be due to the presence of a magnetic field in the experiments(to more accurately reproduce actual thruster conditions). As mentioned previously, the experimental measurements were obtained with a floating keeper and not a keeper current of 1.5A, which corresponds to the NSTAR neutralizer keeper current (3). To see the effect of this, simulations were run with a small keeper current of 20mA and the results indicate that the densities upstream of the orifice are somewhat lowered but remain essentially the same there and further downstream. Except for the measurement before the peak one, the Comsol predictions fall outside the measurements taking into account the published uncertainty estimates(2).

Figure 11 compares the plasma potentials and it can be seen that whist the overall trend of a monotonic increase with axial distance with gradient changes close to and in the orifice, the Comsol predictions of the absolute potential are higher than both the experimental and reference (3) modelling values. Near the orifice, the gradients predicted by the Comsol simulations tend to be lower than either (3) or the experimental ones, while further downstream they seem to more consistent with the experimental values.

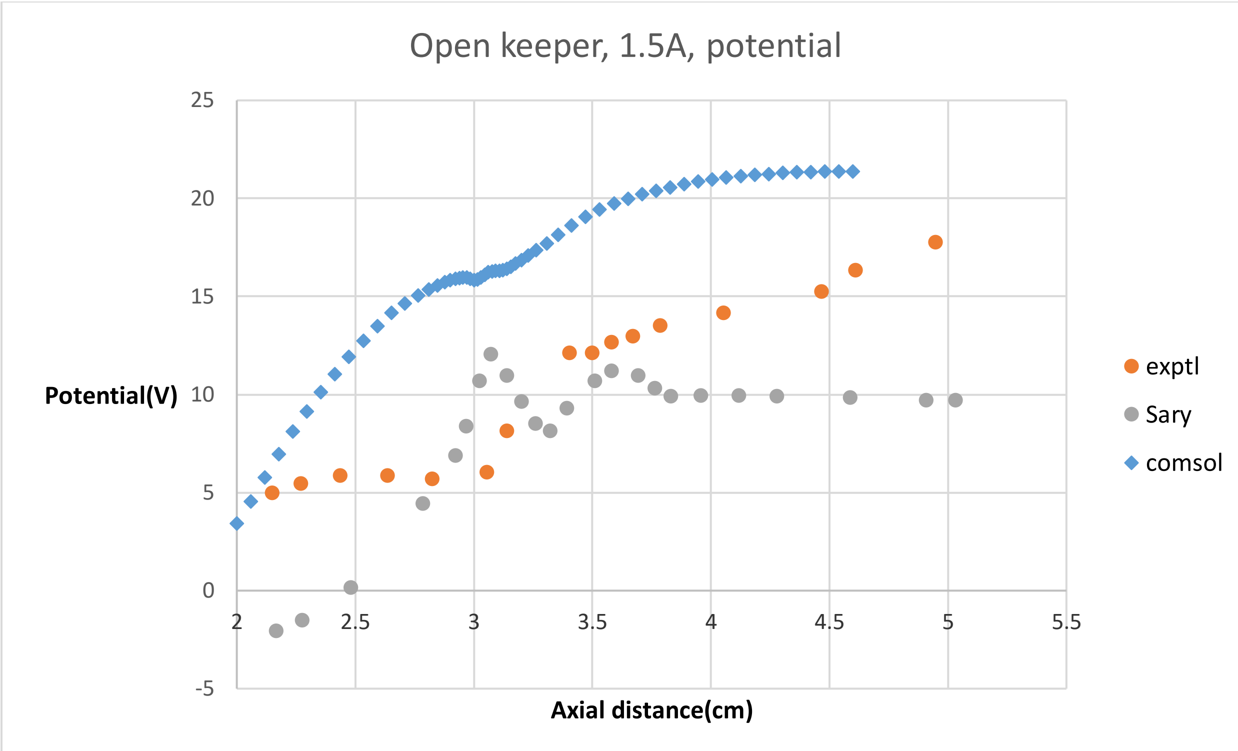

Figure 11. Comparison of potentials on axis

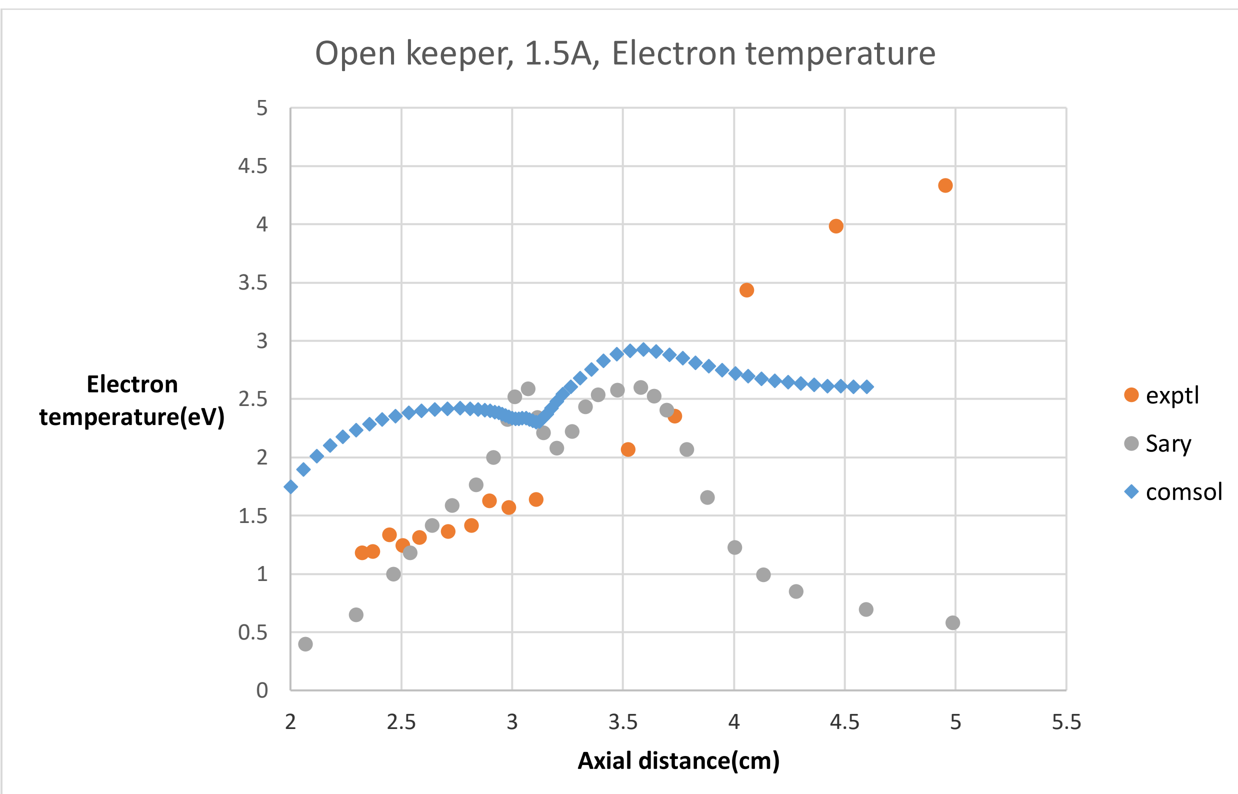

Figure 12. Comparison of electron temperatures on axis

Although, the electron temperature predictions, like the potentials, show the same qualitative behavior as (3) and the experimental values, the absolute values upstream of the orifice entrance are consistently higher than the others. However, at the actual orifice entrance and just beyond, the Comsol results are within about 15% of the Sary ones and from the orifice exit to abut 3.5cm they show the same increase with a very similar gradient.

In order to improve the fidelity of the simulations in terms of the keeper geometry, further modelling was performed using two modified geometries, the first called partially open where the keeper has a cylindrical wall extending upstream but does not close as happens in actual closed keepers, and the second where the keeper is completely closed but with an insulating wall flush with the cathode orifice exit(and not at the upstream end as in actual cathodes), as shown in Figures 13 and 14, respectively. Both modified geometries had significant effects on the on-axis profiles of the plasma parameters. For brevity not all the results are presented here but in summary there was a decrease in the densities up to and including at the orifice, resulting in the Comsol predictions being lower there than both the others, whilst beyond the orifice the values were essentially unchanged and in very good agreement with those from (3). For the potentials and electron temperatures, the values were generally lowered to bring them into closer agreement with both the experimental and Sary prediction values. Figure 15 shows, an example for the closed keeper, where now the plasma potentials are in much better agreement with the Sary model upstream and through the orifice and then in very agreement with the experimental measurements close to and further downstream of the keeper.

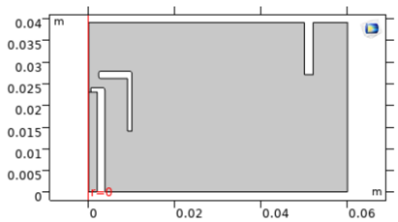

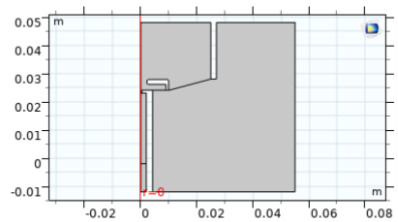

Figure 13. Partially open keeper geometry Figure 14. Closed keeper geometry

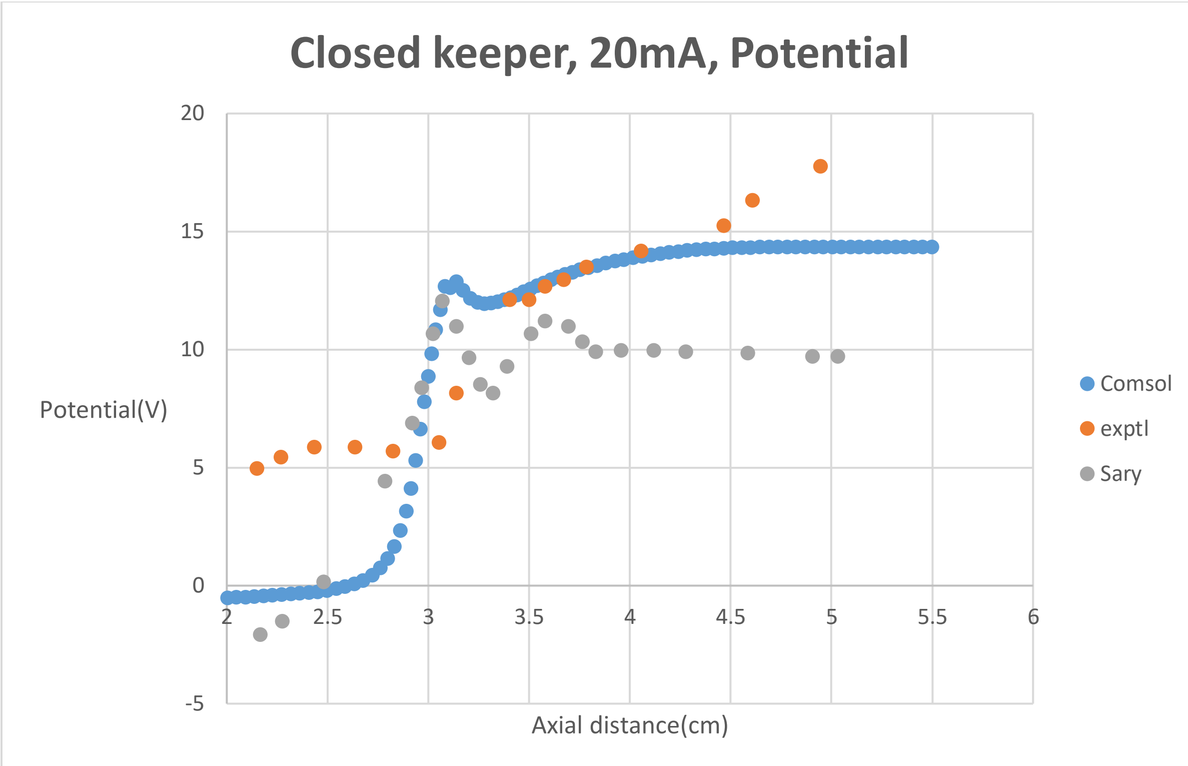

Figure 15. Comparison of potentials on axis for closed keeper geometry

3. Keeper potentials and validation

One of the original motivations of attempting to model hollow cathodes with COMSOL was that of being able to predict the potential on the keeper electrode with inputs only of the mass flow rate and the currents for a given geometry.
Since the majority of the modelling was performed on an NSTAR cathode operating at TH15, it seemed logical to try to predict the keeper potentials for this case. Initially the keeper current was set as 1.5A and the resulting keeper potential was around 11V, which is in reasonably good agreement with the modelling prediction in (4). However, a search was then made to find experimental values of this parameter. This was not so easy to find, but eventually some references were found with experimental values but not in the diode or triode mode and not with a keeper current of 1.5A but in a floating or almost floating mode with the keeper tied to the anode through a 1kohm resistor(6, 7). The keeper potentials measured were significantly lower, around 5V. Reference 4 does indeed mention that their simulations used a keeper current of 1.5A which was that for the NSTAR neutralizer and not the discharge cathode and says that the keeper potential does vary with its current, increasing as the current increases but doesn't really say much as to why. Simulations were then performed with zero current and a small value which would correspond to that when the keeper was connected to the anode through a 1 k Ohm resistor.

The results are shown in Table 3 and it appears that increasing the keeper current for the same geometry increases the keeper potential as expected. Closing the keeper seems to decrease the potential. However, the predicted value which is closer to that measured experimentally seems to be with an open keeper.

Table 3. Keeper potentials

Keeper configuration	Keeper current(A)	Keeper potential(V)	Experimental values(V)
Closed	0.02	-3.75	5.47(cathode flow rate 3.13sccm)(7); ~4 (6)
Partially open	1.5	3.1	-
Open	1.5	11.08	13(4)
Open	0.02	5.31	-

IV. CONCLUSIONS

The COMSOL plasma tool has been used to simulate simplified hollow cathode diode configurations with xenon gas. The 2-D model is in essence a drift diffusion one and includes some plasma chemistry as well as surface reactions at the electrodes. Three species, electrons, singly charged ions and excited neutrals and 6 reactions, including ionization and excitation, were modelled.

Validation of the model was attempted by comparing the variation along the axis of the electron density, plasma potential and electron temperature with the experimental results and modelling of Sary et al for the NSTAR discharge cathode at the nominal TH15 operating condition. The initial results using an open keeper configuration gave good agreement with the peak electron density as measured experimentally near the orifice and downstream of the orifice exit with the Sary model but overestimated the values further upstream of the orifice entrance. For this keeper configuration, whilst the general trends, were reasonably good qualitatively, the absolute values were higher, especially for the potentials. Two other keeper geometries were simulated, one partially open and the other fully closed and although this improved the agreement in the absolute values of plasma potentials and electron temperatures, it tended to underestimate the electron densities.

To further validate the model, comparison was made with measured and predicted keeper potentials for the NSTAR discharge cathode at the TH15 operating point; the results are not easily understood since it seems that the open keeper configuration gave values very close to the measured values despite the rather poor agreement in potentials and electron temperatures. One possible reason for this is the presence of a magnetic field in the experiments and future work will include this effect. Other future activities include, measurement of the keeper potentials over a range of operating conditions for LaB6 cathodes. However, currently the model needs an emitter temperature distribution and the intention is to couple the existing coupled plasma and neutral flow model with a thermal model to get emitter temperature distributions.

One key area that still needs to be improved is that of the neutral flow since currently it is laminar flow throughout whereas in practice there will be regions of transition and free molecular flow. One way of overcoming this would be to use a DMSC model to generate the pressure distributions and then feed this into the plasma tool.

However, the drift diffusion model may not be applicable in any case since the drift-diffusion approximation is suitable when the gas pressure is above about 1.33 Pa and the reduced electric field typically less than 500 Townsends. Additionally, the number density of charged species should be much less than the number density of the neutrals ie the plasma should be weakly ionized. The plasma should also be collisional such that the mean free path between electrons and the neutrals should be much less than the characteristic dimension of the system. While these conditions may be met in some of the regions like the insert and possibly the orifice(or perhaps only the upstream part), further downstream of the orifice exit where the neutral densities are much lower, they may not all be satisfied. This may explain some of the discrepancies between the measured and predicted values of plasma parameters and also keeper potentials. Further calculations will be performed to check if these conditions are met.

References

[1] Ioannis G. Mikellides, Ira Katz, Dan M. Goebel, and James E. Polk "Hollow cathode theory and experiment. II. A two-dimensional theoretical model of the emitter region," Journal of Applied Physics **98**, 113303,2005.
[2] Dan M. Goebel, Kristina K. Jameson, Ron M. Watkins, Ira Katz, and Ioannis G. Mikellides, "Hollow cathode theory and experiment. I. Plasma characterization using fast miniature scanning probes," Journal of Applied Physics **98**, 113302,2005.
[3] Gaétan Sary, Laurent Garrigues and Jean-Pierre Boeuf, "Hollow cathode modelling: I. A coupled plasma thermal two-dimensional model," Plasma Sources Sci. Technol. **26**, 055007, 2017.
[4] Gaétan Sary, Laurent Garrigues and Jean-Pierre Boeuf, "Hollow cathode modelling: II. Physical analysis and parametric study," Plasma Sources Sci. Technol. **26**, 055008, 2017.
[5] Hui Liu, Min Li, Zhongxi Ning, Junxue Ren, Haibin Tang, Daren Yu, Evgenii V. Demidov, Stepan I. Eliseev, and Anatoly A. Kudryavtsev, "2-D Modelling of Orificed Hollow Cathodes of Stationary Plasma Thrusters SPT-100", IEEE Transactions on Plasma Science, Volume: 43, Issue: 12, Dec. 2015.
[6] Matthew T. Domonkos, John E. Foster, and Michael J. Patterson," Investigation of Keeper Erosion in the NSTAR Ion Thruster ", IEPC-01-308, 27th International Electric Propulsion Conference
[7] Daniel A. Herman and Alec D. Gallimore, "Near Discharge Cathode Assembly Plasma Potential Measurements in a 30-cm NSTARtype Ion Engine amidst Beam Extraction", 40th AIAA/ASME/SAE/ASEE Joint Propulsion Conference and Exhibit, 11 - 14 July 2004, Fort Lauderdale, Florida